

PREPARED FOR SUBMISSION TO JCAP

A novel method to extract dark matter parameters from neutrino telescope data

Arman Esmaili^{a,b} Yasaman Farzan^c

^aInstituto de Física Gleb Wataghin - UNICAMP, 13083-859, Campinas, SP, Brazil

^bSchool of Particles and Accelerators, Institute for Research in Fundamental Sciences (IPM), P.O.Box 19395-5531, Tehran, IRAN

^cSchool of Physics, Institute for Research in Fundamental Sciences (IPM), P.O.Box 19395-5531, Tehran, IRAN

E-mail: arman@ipm.ir, yasaman@theory.ipm.ac.ir

Abstract. Recently it has been shown that when the Dark Matter (DM) particles captured in the Sun directly annihilate into neutrino pairs, the oscillatory terms in the oscillation probability do not average to zero and can lead to a seasonal variation as the distance between the Sun and Earth changes in time. In this paper, we explore this feature as a novel method to extract information on the properties of dark matter. We show that by studying the variation of the flux over a few months, it would in principle be possible to derive the DM mass as well as new information on the flavor structure of the DM annihilation modes. In addition to analytic analysis, we present the results of our numerical calculations that take into account scattering and regeneration of neutrinos traversing the Sun.

Contents

1	Introduction	1
2	Neutrino flux from dark matter annihilation in the Sun	2
3	Theoretical motivation	3
4	The IceCube neutrino telescope	4
4.1	General description	4
4.2	Observable quantities at neutrino telescopes	5
4.3	Background	6
5	Numerical calculations	6
6	Analysis of information from seasonal variation	8
7	Illustrative examples	13
8	Conclusion and discussion	16

1 Introduction

If the dark matter is composed of Weakly Interacting Massive Particles (WIMPs), it can be trapped inside the Sun and give rise to a neutrino flux which is in principle detectable at the neutrino telescopes. Detection of such a flux is an indirect way of detecting DM which has received much attention in the recent years. If the flux is high enough, in addition to establishing WIMP as the DM, information on DM annihilation can be derived from the properties of the flux such as energy spectrum or flavor composition.

Recently it has been shown in [1] that if the annihilation to neutrino pairs is one of the dominant modes, the oscillatory terms in the oscillation probability will lead to a seasonal variation of the number of muons produced by the Charged Current (CC) interaction of ν_μ from the Sun in the neutrino telescopes. That is because in this case, the spectrum of neutrinos is monochromatic so, contrary to the general belief, the oscillatory terms do not average to zero and vary throughout a year as the distance between the Sun and Earth changes due to nonzero eccentricity of the Earth's orbit. As pointed out in [1], the seasonal variation can be considered as an independent tool to derive information on the DM annihilation modes. In this paper, we further elaborate on this possibility. We analyze the information that can be derived from this observable on the flavor structure of DM annihilation amplitude. We also present numerical results using a code that solves evolution equations describing the neutrino propagation, taking into account the effects of neutrino absorption, scattering and ν_τ regeneration inside the sun.

Our particular attention is given to the case that DM particles primarily annihilate into neutrinos. As has been discussed in detail in ref. [2], wide classes of models can be built in which the dominant annihilation mode of DM particles is the annihilation into neutrinos. At first sight it might seem that within such models, the DM interactions with nuclei will be too weak to give rise to a substantial DM abundance in the Sun center and thus to a significant

neutrino flux. We briefly discuss this issue and show that, despite dominantly annihilating into neutrinos, DM can have large enough spin-dependent scattering cross section off the protons inside the Sun. Our main approach in this paper is however model independent. Our goal is to find out to what extent the properties of DM (e.g., $\text{Br}(\text{DM} + \text{DM} \rightarrow \nu_\alpha \nu_\beta)$) can be determined by combining the information on seasonal variation and on flavor composition (more precisely, the ratio of the detected muon-like events to shower-like events).

This paper is organized as follows. In section 2, the general properties of the flux is described and the seasonal variation is quantified. In section 3, the theoretical framework within which a DM pair dominantly annihilates to a neutrino pair is discussed and shown that the DM capture rate in the Sun and the subsequent neutrino flux can be high enough to make the method presented in this paper viable. In section 4, the properties and limitation of neutrino detectors are described and the observable quantities are formulated. In section 5, the numerical code that has been developed to carry out the calculation is described. In section 6, the information that can be in principle derived from the observable quantities defined in the previous sections on the flavor structure of DM interactions are analyzed. In section 7, numerical results are presented and the observed patterns are analyzed. Concluding remarks are given in section 8.

2 Neutrino flux from dark matter annihilation in the Sun

DM particles propagating in the space between stars and planets in the galaxy can enter the compact objects such as the Sun or the Earth. If the scattering cross section of DM off nuclei is large enough, these particles can lose energy at scattering and fall into the gravitational potential of the Sun or the Earth. As a result, the DM particles will be accumulated in the center. The accumulated DM particles annihilate with each other and produce the Standard Model (SM) particles. Among the SM particles only neutrinos can reach the surface from the Sun or Earth center. The rest will either be trapped or decay before reaching the surface. DM annihilation can give rise to a neutrino flux either directly (i.e., $\text{DM} + \text{DM} \rightarrow \nu\nu$) or as secondaries (i.e., $\text{DM} + \text{DM} \rightarrow X\bar{X}$ and subsequently $X \rightarrow \nu Y$). If the mass of the DM particles is above a few hundred GeV, the neutrino flux from the DM annihilation can be detectable at the neutrino telescopes such as IceCube. The number of the neutrino events at IceCube produced by DM annihilation in the Sun center can be of the order of a few hundred events per year. The background neutrinos pointing towards the Sun is below 100 events per year [3–5], so the detection of an excess of these neutrinos at these energy ranges can be interpreted as a conclusive indirect detection of DM.

Depending on the couplings and characteristics of the DM particles, the flavor composition and the energy spectrum of the neutrino flux can be different. In particular, if neutrinos are secondaries, we expect a continuous spectrum. On the contrary, if DM particles annihilate directly into neutrinos, the neutrino energy spectrum at production point will be monochromatic. That is because the DM particles annihilate non-relativistically. In fact, the thermal motion of DM particles can widen the line to a very narrow Gaussian with width $\delta E/E \sim 10^{-4}$ [1]. Propagation of the monochromatic neutrinos from the dark matter annihilation in the Sun has been studied in a number of papers including in [7–9]. This difference in spectrum can in principle be invoked to discriminate between the scenarios predicting different decay modes. Ref. [6] has systematically studied the possibility to extract $\text{Br}(\text{DM} + \text{DM} \rightarrow \nu\nu)$ and $\text{Br}(\text{DM} + \text{DM} \rightarrow \tau\bar{\tau})$ by measuring the energy spectrum.

The spectrum of neutrinos emerging from the Sun surface will consist of a sharp line, corresponding to un-scattered neutrinos, superimposed on a continuous tail corresponding to scattered or regenerated neutrinos. The sharp line can still give rise to oscillatory behavior which is the base of the method suggested in this paper to determine if $(\text{DM} + \text{DM} \rightarrow \nu\nu)$ is among the dominant annihilation modes. Following ref. [1], we define the seasonal variation, Δ , as

$$\Delta(t_1, \Delta t_1; t_2, \Delta t_2) \equiv \frac{\tilde{N}(t_1, \Delta t_1) - \tilde{N}(t_2, \Delta t_2)}{\tilde{N}(t_1, \Delta t_1) + \tilde{N}(t_2, \Delta t_2)} \quad (2.1)$$

where

$$\tilde{N}(t, \Delta t) \equiv \frac{\int_t^{t+\Delta t} (dN_\mu/dt) dt}{\int_t^{t+\Delta t} A_{eff}(\theta[t]) L^{-2}(t) dt} \quad (2.2)$$

in which L is the distance between the Sun and the Earth and $A_{eff}(\theta[t])$ is the effective area of the detector which depends on the angle between the beam direction and the axis of the detectors, $\theta(t)$. As the Earth orbits around the Sun, L and θ both change with time during a year. Notice that with this definition, the $1/L^2$ dependence of the flux does not affect Δ . Δ vanishes when the oscillatory terms are absent or averaged out. As shown in [1], Δ can be substantially large and exceed 50 % so with a moderate accuracy, its nonzero value, which is a proof of the existence of the mode $(\text{DM} + \text{DM} \rightarrow \nu\nu)$ can be established. The value of Δ depends on the DM mass, $\text{Br}(\text{DM} + \text{DM} \rightarrow \nu\nu)$ and the initial flavor composition as well as neutrino oscillation parameters. As pointed out in ref. [1], the value Δ can be used to extract information on the initial flavor composition, especially when it is combined with energy spectrum measurements. Of course, to construct Δ , the chosen intervals, Δt_1 and Δt_2 , should not be too small. Otherwise, the statistics will be too low, making the derivation of Δ meaningless due to the large statistical error. For the energy interval of our interest (*i.e.*, $E_\nu \sim 100 - 500$ GeV) even if we take $\Delta t_1 + \Delta t_2 = 1$ year, the oscillatory terms do not average out. Even the oscillatory terms corresponding to Δm_{31}^2 survive. We will elaborate on this point later on. Considering this fact, there is practically no upper bound on Δt_i , except that $\Delta t_1 + \Delta t_2 < 1$ year.

3 Theoretical motivation

As discussed in ref. [1], in order to have non-vanishing Δ , the following two conditions are necessary: (1) The neutrino spectrum has to include a sharp line with width $\delta E/E \ll 4\pi E/(\Delta m^2 L)$ which can be realized if the DM annihilation into neutrino pair is significant; (2) the neutrino flux at production must be non-democratic; *i.e.*, $F_{\nu_e}^0 : F_{\nu_\mu}^0 : F_{\nu_\tau}^0 \neq 1 : 1 : 1$. We have already discussed the reason for the first condition. The second condition is also necessary because for $F^0 \equiv F_{\nu_e}^0 = F_{\nu_\mu}^0 = F_{\nu_\tau}^0$, the neutrino flux at Earth will be independent of the oscillation probability ($F_{\nu_\beta} = \sum_\alpha F_{\nu_\alpha}^0 P(\nu_\alpha \rightarrow \nu_\beta) = F^0 \sum_\alpha P(\nu_\alpha \rightarrow \nu_\beta) = F^0$) and as a result, Δ will vanish because it comes from the oscillatory terms in the oscillation probability.

As discussed in ref. [2], various classes of models can be built that satisfy both these conditions. An explicit example is given in ref. [10]. In order to measure Δ , the number of collected neutrino events has to be larger than a few hundred. If the flux is close to the upper bound from AMANDA, such an amount of data can be collected at IceCube. For $m_{DM} \sim 100$ GeV, the neutrino emission from the Sun with a rate of order of 10^{20} sec^{-1} will be enough to lead to a few hundred events per year. In the saturation limit where the

capture rate of DM particles by the Sun, C_\odot , equals the neutrino emission rate (i.e., two times the annihilation rate), the neutrino emission rate can be translated into a bound on the DM-nuclei cross section. As seen from eqs. (9.25) and (9.26) of [11], for spin-independent scattering mediated by a scalar, with a DM-nucleon cross section, σ_n , as small as 10^{-9} pb, $C_\odot = 10^{20} \text{ sec}^{-1}$ can be achieved. Such cross section is below the present bound on spin-independent DM-nucleon cross section [12]. It is noteworthy that while the Sun is mainly composed of protons, for spin-independent interactions, the heavier nuclei inside the Sun play the dominant role in capturing the DM particles. That is because the nucleons in a nucleus interact coherently with DM so the cross section grows quadratically with nucleus mass. If the DM-quark interaction is mediated via a heavy scalar, we would have

$$\frac{\langle \sigma(\text{DM} + \text{DM} \rightarrow q\bar{q})v \rangle|_{\text{decoupling}}}{\sigma_n} \sim \left(\frac{m_p + m_{DM}}{m_p} \right)^2 \sim 10^4. \quad (3.1)$$

Thus, $\langle \sigma(\text{DM} + \text{DM} \rightarrow q\bar{q})v \rangle|_{\text{decoupling}} \sim 10^{-5} \text{ pb} \ll \langle \sigma_{tot}v \rangle \sim 1 \text{ pb}$. The above discussion shows that it is possible to construct a model within which DM-nucleus interaction is large enough for sufficient DM capture in the Sun but at the same time, the main annihilation mode of DM pairs is the annihilation into neutrino pairs.

4 The IceCube neutrino telescope

4.1 General description

IceCube is a km^3 -scale neutrino telescope recently completed at the south pole [13]. IceCube, which encompasses the AMANDA experiment [14], has been designed to detect the flux of galactic and extragalactic neutrinos with energies higher than a few 10 GeV. The detector consists of 80 strings, each carrying 60 photo-multiplier tubes (PMT) which are being deployed between 1450 m and 2450 m depth. In addition, there are six more strings with a denser array of PMTs between 1760 m and 2450 m, which with the surrounding strings constitute the DeepCore detector at the far depth of the IceCube. Since the PMTs at the DeepCore are closer, the sensitivity of DeepCore is higher than the rest of IceCube and its detection threshold is lower. As explained later, the background events at the DeepCore are also highly suppressed such that, in spite of the small volume of DeepCore which reduces the statistics of the signal, the discovery chance can still be comparable to that by the whole IceCube.

For neutrinos with energy $\mathcal{O}(100 \text{ GeV})$, IceCube cannot distinguish between the neutrino flavors completely. Practically, IceCube can identify two types of events: μ -track and shower-like events. Let us explain them one by one. The μ -track events are the Cherenkov radiation collected by the PMTs when a muon passes through the instrumented volume of the detector. The muons can be produced in two ways: i) from the CC interaction of ν_μ and $\bar{\nu}_\mu$; ii) from CC interactions of ν_τ (and $\bar{\nu}_\tau$) which produces the tau (and the anti-tau) particle and the subsequent $\tau^- \rightarrow \mu^- \bar{\nu}_\mu \nu_\tau$ (and $\tau^+ \rightarrow \mu^+ \nu_\mu \bar{\nu}_\tau$). However, the small branching ratio of the tau particle's leptonic decay, $\text{Br}(\tau \rightarrow \mu \nu \nu) = 17\%$, makes the contribution from ν_τ and $\bar{\nu}_\tau$ subdominant. Thus, the number of μ -track events is practically given by the fluxes of ν_μ and $\bar{\nu}_\mu$ incident on the IceCube. Considering the position of the muon production point, the μ -track events for the whole IceCube can be divided into two categories: i) Through-going μ -track events for which the muons are produced inside or in the vicinity of the instrumented volume of the detector; ii) Contained μ -track events for which the production point

is within the geometrical volume of the detector. Similar consideration also holds for the muon neutrinos detected at the DeepCore. In fact, tracks originated inside the IceCube (but outside DeepCore) and passing through the DeepCore will count as “through-going” events for DeepCore and as “contained” events for IceCube.

The second type of events that can be identified at the IceCube is the shower-like events which are nearly spherical volumes of Cherenkov radiation from the hadronic or electromagnetic cascades. The interactions contributing to the shower-like events consist of: i) Neutral Current (NC) interaction of all the three neutrinos flavors ν_α and $\bar{\nu}_\alpha$; ii) CC interaction of ν_e and $\bar{\nu}_e$; iii) CC interaction of ν_τ and $\bar{\nu}_\tau$, and the accompanying hadronic decay of the produced tau particle. The event rate calculation of these interactions can be found in [15].

4.2 Observable quantities at neutrino telescopes

In this subsection, we quantify the observable quantities that we shall use in our subsequent analysis; namely, the seasonal variation and the ratio of μ -track events to shower-like events. We define two versions of the observable $\Delta(t_1, \Delta t_1; t_2, \Delta t_2)$ in eq. (2.1).

- The $\Delta^{\text{IC}}(t_1, \Delta t_1; t_2, \Delta t_2)$ is the seasonal variation of the through-going μ -track events for the whole IceCube. To compute Δ^{IC} , we calculate the number of μ -track events (per unit of time) with the following formula

$$\begin{aligned} \frac{dN_\mu^{\text{IC}}}{dt} &= \int_{E_{\text{thr}}}^{m_{DM}} \int_{E_{\text{thr}}}^{E_{\nu_\mu}} \frac{d\Phi_{\nu_\mu}}{dE_{\nu_\mu}} \left[\frac{d\sigma_{\nu p}^{CC}}{dE_\mu}(E_{\nu_\mu})\rho_p + \frac{d\sigma_{\nu n}^{CC}}{dE_\mu}(E_{\nu_\mu})\rho_n \right] \\ &\times A_{\text{eff}}(E_\mu, \theta[t]) (R_\mu(E_\mu, E_{\text{thr}}) + d) dE_\mu dE_{\nu_\mu} + (\nu_\mu \rightarrow \bar{\nu}_\mu), \end{aligned} \quad (4.1)$$

where $d\Phi_{\nu_\mu}/dE_{\nu_\mu}$ is the flux of ν_μ at the IceCube site, $d\sigma_{\nu p}^{CC}/dE_\mu$ and $d\sigma_{\nu n}^{CC}/dE_\mu$ are the scattering CC partial cross section of muon neutrinos off proton and neutron respectively, $\rho_p \sim 5/9N_A \text{ cm}^{-3}$ and $\rho_n \sim 4/9N_A \text{ cm}^{-3}$ are the number densities of protons and neutrons in the vicinity of the IceCube in terms of Avogadro’s number N_A , R_μ is the muon range in the ice [16], and $d = 1 \text{ km}$ is the size of IceCube. A_{eff} , which is given in appendix of [17], is the IceCube’s effective area of muon detection and depends on the zenith angle of the arriving neutrinos $\theta[t]$. Finally, The E_{thr} is the energy threshold of muon detection at the IceCube which we have set equal to 40 GeV [17]. Notice that in writing eq. (4.1), we have taken into account the fact that the maximum E_μ equals E_{ν_μ} .

- The second version of the observable defined in eq. (2.1) is $\Delta^{\text{DC}}(t_1, \Delta t_1; t_2, \Delta t_2)$ corresponding to the seasonal variation of the DeepCore μ -track events. The number of μ -track events determining Δ^{DC} is given by

$$\begin{aligned} \frac{dN_\mu^{\text{DC}}}{dt} &= \int_{E_{\text{thr}}}^{m_{DM}} \int_{E_{\text{thr}}}^{E_{\nu_\mu}} \frac{d\Phi_{\nu_\mu}}{dE_{\nu_\mu}} \left[\frac{d\sigma_{\nu p}^{CC}}{dE_\mu}(E_{\nu_\mu})\rho_p + \frac{d\sigma_{\nu n}^{CC}}{dE_\mu}(E_{\nu_\mu})\rho_n \right] \\ &\times V_{\text{eff}}^{\text{DC}}(E_\mu) dE_\mu dE_{\nu_\mu} + (\nu_\mu \rightarrow \bar{\nu}_\mu), \end{aligned} \quad (4.2)$$

where V_{eff}^{DC} is the effective volume of the DeepCore given by [5]

$$V_{eff}^{DC}(E_\mu) = (0.0056 \log E_\mu + 0.0146) \Theta(275 - E_\mu) + 0.0283 \Theta(E_\mu - 275), \quad (4.3)$$

in which $\Theta(x)$ is the Heaviside step function and E_μ is in GeV unit. We have set also the energy threshold of the muon detection at the DeepCore equal to 40 GeV [18].

In order to employ the shower-like events in our analysis, we define the following observable

$$R \equiv \frac{\text{Number of } \mu\text{-track events}}{\text{Number of shower-like events}}. \quad (4.4)$$

Similar to the observable Δ , we define two quantities R^{IC} and R^{DC} corresponding to the through-going and DeepCore events respectively. In the case of R^{IC} , the numerator of eq. (4.4) will be calculated using eq. (4.1) and for the denominator we use the geometrical volume of the whole IceCube detector. Similarly, for the calculation of the numerator of R^{DC} we use eq. (4.2); while in the denominator we use the geometrical volume of the DeepCore. Generally, if $E_{thr}^{shower} \geq m_{DM}$, where E_{thr}^{shower} is the energy threshold for the detection of shower-like events, there will be no shower-like events at the detector. To carry out this analysis, we set E_{thr}^{shower} equal to 100 GeV. This assumption is rather optimistic as in reality $E_{thr}^{shower} \sim 1$ TeV. However, in this paper our main focus is on Δ which does not employ shower-like events. If no practical way to improve E_{thr}^{shower} is found, there will be even more motivation for pursuing the measurement of Δ .

4.3 Background

In the measurement of both observables Δ and R at the IceCube, the background events should be considered. The two main sources of backgrounds at the IceCube are atmospheric muons and atmospheric neutrinos. The atmospheric muons are isotropically produced in the collision of the cosmic rays with the atmosphere. However, from March equinox to September equinox (corresponding to spring and summer in the northern hemisphere) when the Sun is below the horizon, the Earth acts as a filter for the atmospheric muons so these backgrounds will be suppressed. Thus, for the through-going events at the IceCube we integrate eq. (4.1) over the March to September period of the year. For the DeepCore, the instrumented volume of the IceCube surrounding it acts as a veto (up to one part in 10^6 [18, 19]) so it is possible to take data at DeepCore throughout the whole year. Thus, we calculate the number of muon-track events at the DeepCore by integrating eq. (4.2) over the whole year. The other source of backgrounds, atmospheric neutrinos, can be suppressed thanks to the high angular resolution of the IceCube in the μ -track reconstruction (about 1° [19]). Considering only the events in a cone with half angle 1° around the position of the Sun will reduce the number of through-going atmospheric neutrino backgrounds to ~ 6 events per year ($\sim 3 \text{ yr}^{-1}$ for DeepCore). There is also an irreducible background from the solar atmospheric neutrinos but the flux is expected to be low [3].

5 Numerical calculations

As mentioned in section 1, the neutrinos at the center of Sun are monochromatic with energy equal to the DM particle mass. However, due to the NC and CC interaction of the neutrinos with the Sun medium, the spectrum of the neutrinos emerging from the surface of the Sun,

in addition to the sharp line of the monochromatic neutrinos, will contain a continuous tail corresponding to the scattered or regenerated neutrinos. We have written a Mathematica code to numerically compute the flux of neutrinos at the surface of the Sun. In the code we have taken into account the oscillation of the neutrino flavors in the Sun medium, CC and NC interactions of the neutrinos with the nuclei, and the neutrinos coming from the tau regeneration effect.

Flavor oscillation of the neutrinos in the Sun medium has been computed using the updated matter density profile of the Sun $n_e(r)$ from ref. [20]. The oscillation Hamiltonian is

$$\mathcal{H}_{\text{osc}} = \frac{(M^2)_{\text{diag}}}{2E_\nu} + \text{diag}(\sqrt{2}G_F n_e, 0, 0), \quad (5.1)$$

where E_ν is the neutrino energy, G_F is the Fermi constant and

$$(M^2)_{\text{diag}} = U^\dagger M_\nu^2 U = \text{diag}(-\Delta m_{12}^2, 0, \xi \Delta m_{32}^2).$$

M_ν is the neutrino mass matrix and U is the PMNS unitary mixing matrix. The parameter ξ takes values +1 and -1, respectively corresponding to the normal and inverted neutrino mass schemes. For the mixing parameters we insert $\Delta m_{12}^2 = 8.0 \times 10^{-5} \text{ eV}^2$, $\Delta m_{32}^2 = 2.4 \times 10^{-3} \text{ eV}^2$, $\theta_{12} = 33.46^\circ$ and $\theta_{23} = 45^\circ$, $\theta_{13} = 0$ and 7° , $\delta = 0, \pi/2$ and π .

For the NC and CC interaction cross sections we have used the tabulated values from ref. [21]. The NC interaction of a neutrino flavor lowers the energy of the neutrino without changing the flavor. The CC interaction of $\bar{\nu}_e^{(-)}$ and $\bar{\nu}_\mu^{(-)}$ transforms them into the corresponding charged leptons and therefore reduces the neutrino flux. The tau and anti-tau particles created by the CC interactions of ν_τ and $\bar{\nu}_\tau$ promptly decay and reproduce neutrinos (“tau regeneration”). For example, the decay of the tau particle through the channel $\tau^- \rightarrow \mu^- \bar{\nu}_\mu \nu_\tau$ reinject $\bar{\nu}_\mu$ and ν_τ with lower energy into the flux of neutrinos. We consider the following decay channels for the tau particle: $\text{Br}(\tau \rightarrow e \nu_e \nu_\tau) = 0.18$, $\text{Br}(\tau \rightarrow \mu \nu_\mu \nu_\tau) = 0.18$, $\text{Br}(\tau \rightarrow \pi \nu_\tau) = 0.12$, $\text{Br}(\tau \rightarrow a_1 \nu_\tau) = 0.13$, $\text{Br}(\tau \rightarrow \rho \nu_\tau) = 0.26$ and $\text{Br}(\tau \rightarrow \nu_\tau X) = 0.13$. As can be seen, tau regeneration couples the evolution equations of different flavors together (it also couples the neutrino flux evolution to the anti-neutrino evolution). The details of the tau regeneration calculation as well as the neutrino spectra in the above decay channels can be found in [22]. The set of coupled evolution equations describing the neutrino propagation can be found in [9].

Let us take the state of the neutrinos at the production point to be $|\nu_\alpha\rangle$. By solving the evolution equations numerically, we obtain the state of the neutrinos $|\nu_\alpha; \text{surface}\rangle$ at the surface of the Sun. After leaving the Sun, neutrinos will propagate through the empty space towards the Earth. The evolution of the state $|\nu_\alpha; \text{surface}\rangle$ from the Sun surface to the Earth is given simply by multiplying each mass eigenstate with phases, $\exp[i m_i^2 L / E_\nu]$. These phases depend on the distance between the Sun and Earth (i.e., L) which is a function of time. Considering the eccentricity of the Earth’s orbit around the Sun and also the tilt of the Earth’s rotation axis with respect to the ecliptic plane, we have calculated $\theta(t)$ and $L(t)$ during a year (see eq. 2.1 and 2.2). After calculating the values of $\theta(t)$, $L(t)$ and the spectrum of neutrinos arriving at Earth during the year, we have computed the observables R and Δ according to the formulation presented in section 4.

It should be mentioned that the flux of neutrinos arriving in the Earth has been calculated previously by Blennow et al. [8] for different annihilation modes of DM and the mixing parameters $\theta_{13} = 0, 5^\circ, 10^\circ$ and $\delta = 0$. However, since we needed the flux of neutrinos

for other values of the mixing parameters (especially $\delta = 0, \pi/2$ and π), we have calculated it independently. With the same input values of the mixing parameters, our results are in complete agreement with the results of [8].

6 Analysis of information from seasonal variation

Let us take the amplitude of $\text{DM} + \text{DM} \rightarrow \nu_\alpha + \overset{(-)}{\nu}_\beta$ to be $\mathcal{M}_{\alpha\beta}$. The state resulting from the DM pair annihilation will be a “pure” coherent state of type $|\psi\rangle = \sum_{\alpha\beta} \mathcal{M}_{\alpha\beta} |\nu_\alpha(\vec{p}_1) \overset{(-)}{\nu}_\beta(\vec{p}_2)\rangle$.

The density matrix is $|\psi\rangle\langle\psi| = \sum_{\alpha\beta\gamma\sigma} \tilde{\rho}_{\alpha\beta,\gamma\sigma} |\nu_\alpha \overset{(-)}{\nu}_\beta\rangle\langle\nu_\gamma \overset{(-)}{\nu}_\sigma|$ in which $\tilde{\rho}_{\alpha\beta,\gamma\sigma} = \mathcal{M}_{\alpha\beta} \mathcal{M}_{\gamma\sigma}^*$. Since the DM pairs are almost at rest inside the Sun, the momenta of the produced pair will be opposite to each other (i.e., $\vec{p}_1 \simeq -\vec{p}_2$) which means at most one of the emitted neutrinos will reach the earth. As a result, the density matrix of the neutrinos pointing towards us will be the following “reduced” matrix

$$\rho_{\alpha\beta} |\nu_\alpha\rangle\langle\nu_\beta| \quad \text{with} \quad \rho_{\alpha\beta} = \sum_{\gamma} \tilde{\rho}_{\alpha\gamma,\beta\gamma} = (\mathcal{M} \mathcal{M}^\dagger)_{\alpha\beta} .$$

Notice that although the two particle state $|\psi\rangle$ is pure (i.e., $\tilde{\rho} \log \tilde{\rho} = 0$), the neutrino states reaching the detector are not in general pure (i.e., $\rho \log \rho \neq 0$). In case that the annihilation is lepton number violating $\text{DM} + \text{DM} \rightarrow \nu_\alpha + \nu_\beta$, $\mathcal{M}_{\alpha\beta}$ is obviously symmetric. As a result, ρ yields $\mathcal{M}_{\alpha\beta}$; i.e., for $\rho = V \rho_{diag} V^\dagger$ where V is a unitary matrix, $\mathcal{M} = V(\rho_{diag})^{1/2} V^T$. In case that the DM annihilation is lepton number conserving (i.e., $\text{DM} + \text{DM} \rightarrow \nu_\alpha \bar{\nu}_\beta$), up to subdominant (or perhaps zero) CP-violating effects, we can write $\mathcal{M}_{\alpha\beta} = \mathcal{M}_{\beta\alpha}^*$. Under this condition, $\mathcal{M}_{\alpha\beta}$ can be again derived from ρ : for a Hermitian \mathcal{M} , $\rho = V \rho_{diag} V^\dagger$ yields $\mathcal{M} = V(\rho_{diag})^{1/2} V^\dagger$. From $\mathcal{M}_{\alpha\beta}$, information on flavor structure of the couplings of DM can be derived. By studying the neutrino flux there is however no way to figure out whether the DM annihilation is lepton number violating or conserving. In the following, we discuss the possibility of constraining ρ from the observable quantities like R and Δ .

The density matrix ρ can be diagonalized as

$$\rho = \sum_{\alpha} n_{\alpha} |\nu'_\alpha\rangle\langle\nu'_\alpha| \quad (6.1)$$

where $\alpha = 1, 2, 3$, $n_{\alpha} \geq 0$ and $\langle\nu'_\alpha|\nu'_\beta\rangle = \delta_{\alpha\beta}$. Notice that ν'_α can in general be different from mass eigenstates ν_1, ν_2 and ν_3 as well as from flavor eigenstates ν_e, ν_μ and ν_τ .

Once ν'_α arrives at the surface of the Sun, it will be a different state that can in general be written in terms of the vacuum mass eigenstates as

$$|\nu'_\alpha; \text{surface}\rangle = a_{\alpha 1}|1\rangle + a_{\alpha 2}|2\rangle + a_{\alpha 3}|3\rangle . \quad (6.2)$$

We do not a priori know what is the flavor composition of ν'_α , so $a_{\alpha i}$ are unknown. A general neutrino state $|\psi\rangle$ produced at the Sun center, while crossing the Sun, evolves into $|\psi; \text{surface}\rangle$ as follows

$$|\psi; \text{surface}\rangle = W(t_P, t_S) |\psi\rangle \quad \text{with} \quad W(t_P, t_S) = \prod_{t_P}^{t_S} \mathcal{T}[1 + iH(t)dt]$$

where t_P and t_S are respectively the production time and the time that neutrino reaches the surface and \mathcal{T} denotes time ordering. Regardless of the time dependence of H , the evolution matrix is unitary so for any arbitrary states $|\psi\rangle$ and $|\chi\rangle$

$$\langle\chi; \text{surface}|\psi; \text{surface}\rangle = \langle\chi|\psi\rangle.$$

As a result, the $|\nu'_\alpha\rangle$ states after evolving in time remain perpendicular:

$$\langle\nu'_\alpha; \text{surface}|\nu'_\beta; \text{surface}\rangle = \sum_i a_{\alpha i} a_{\beta i}^* = \delta_{\alpha\beta}.$$

Thus, the knowledge of two rows of the 3×3 matrix, $a_{\alpha i}$, is enough to determine the matrix $a_{\alpha i}$.

On the way to the Earth, the state will evolve into¹

$$|\nu'_\alpha; \text{detector}\rangle = a_{\alpha 1}|1\rangle + a_{\alpha 2}e^{i\Delta_{12}}|2\rangle + a_{\alpha 3}e^{i\Delta_{13}}|3\rangle, \quad (6.3)$$

in which $\Delta_{ij} \equiv \Delta m_{ij}^2 L / (2E)$. Obviously, the number of μ -tracks and therefore both Δ and R depend on $\sum_\alpha n_\alpha P(\nu_\alpha \rightarrow \nu_\mu)$. Let us then discuss these oscillation probabilities

$$P(\nu_\alpha \rightarrow \nu_\mu) = \sum_i |a_{\alpha i}|^2 |U_{\mu i}|^2 + \quad (6.4)$$

$$2\Re[a_{\alpha 1}^* a_{\alpha 2} U_{\mu 1} U_{\mu 2}^* e^{i\Delta_{12}}] + 2\Re[a_{\alpha 1}^* a_{\alpha 3} U_{\mu 1} U_{\mu 3}^* e^{i\Delta_{13}}] + 2\Re[a_{\alpha 2}^* a_{\alpha 3} U_{\mu 2} U_{\mu 3}^* e^{i(\Delta_{13} - \Delta_{12})}].$$

As shown in ref. [1], the first oscillatory term given by $\exp[i\Delta_{12}]$ does not vanish as we integrate on time over a year when the Earth orbits around the Sun. This term results in sizeable seasonal variation. Changing the DM mass, which coincides with the energy of neutrino line, this term rapidly oscillates with period

$$\frac{\delta m_{DM}}{m_{DM}} = \frac{4\pi m_{DM}}{\Delta m_{21}^2 L} = 0.04 \frac{m_{DM}}{200 \text{ GeV}}. \quad (6.5)$$

It is noteworthy that even the effects of the phase Δ_{13} do not completely vanish. The reason is that due to angular momentum conservation, the Earth slows down when it is at the aphelion so the eccentricity of the orbit gives rise to non-vanishing average. To quantify this claim, let us define

$$O_{12}(t, \Delta t) \equiv \frac{\int_t^{t+\Delta t} e^{i\Delta_{12}(t)} A_{eff}(t) L^{-2}(t) dt}{\int_t^{t+\Delta t} A_{eff}(t) L^{-2}(t) dt}, \quad (6.6)$$

and

$$O_{13}(t, \Delta t) \equiv \frac{\int_t^{t+\Delta t} e^{i\Delta_{13}(t)} A_{eff}(t) L^{-2}(t) dt}{\int_t^{t+\Delta t} A_{eff}(t) L^{-2}(t) dt}. \quad (6.7)$$

For $E_\nu \sim 100 \text{ GeV}$, $|O_{12}| \sim 1$ and $|O_{13}| \sim 0.1$ which means even the effects driven by Δ_{13} do not completely average out. The average oscillation probability can be written as

$$\langle P(\nu_\alpha \rightarrow \nu_\mu) \rangle_t^{t+\Delta t} \equiv \frac{\int_t^{t+\Delta t} P(\nu_\alpha \rightarrow \nu_\mu) A_{eff} L^{-2}(t) dt}{\int_t^{t+\Delta t} A_{eff} L^{-2}(t) dt} =$$

¹The Earth matter effect is irrelevant because for this energy range, the effective mixing is negligible [1].

$$\sum_i |a_{\alpha i}|^2 |U_{\mu i}|^2 + 2\Re[a_{\alpha 1}^* a_{\alpha 2} U_{\mu 1} U_{\mu 2}^* O_{12}] + \mathcal{O}(a_{\alpha i}^2 U_{\mu i}^2 O_{13}). \quad (6.8)$$

Let us now discuss the antineutrinos. The density matrix of antineutrinos at production can be written as

$$\bar{\rho}_{\alpha\beta} |\bar{\nu}_\alpha\rangle\langle\bar{\nu}_\beta| \quad \text{with} \quad \bar{\rho}_{\alpha\beta} \equiv \sum_\gamma \tilde{\rho}_{\gamma\alpha,\gamma\beta} = (\mathcal{M}^T \mathcal{M}^*)_{\alpha\beta}. \quad (6.9)$$

The density matrix $\bar{\rho}$ can be diagonalized as follows

$$\bar{\rho} = \sum_\alpha n_\alpha |\bar{\nu}'_\alpha\rangle\langle\bar{\nu}'_\alpha|. \quad (6.10)$$

Notice that for the lepton number and CP conserving annihilation ($\text{DM} + \text{DM} \rightarrow \nu\bar{\nu}$) with $\mathcal{M} = \mathcal{M}^\dagger$, we find $\rho = \bar{\rho}^*$. On the other hand, for lepton number violating annihilation ($\text{DM} + \text{DM} \rightarrow \nu + \nu, \bar{\nu} + \bar{\nu}$) with $\mathcal{M} = \mathcal{M}^T$, we find $\rho = \bar{\rho}$. In any case n_α in eq. (6.1) for neutrinos and the one in eq. (6.10) for antineutrinos are the same. Moreover, $|\nu'_\alpha\rangle$ and $|\bar{\nu}'_\alpha\rangle$ at the source are the charged conjugate of each other. However, the matter effects on $|\nu'_\alpha\rangle$ and $|\bar{\nu}'_\alpha\rangle$ are different so $|\bar{\nu}'_\alpha; \text{surface}\rangle$ will not in general be the charged conjugate of $|\nu'_\alpha; \text{surface}\rangle$.

Let us expand the antineutrino state $\bar{\nu}'_\alpha$ at the surface as

$$|\bar{\nu}'_\alpha; \text{surface}\rangle = \bar{a}_{\alpha 1} |\bar{1}\rangle + \bar{a}_{\alpha 2} |\bar{2}\rangle + \bar{a}_{\alpha 3} |\bar{3}\rangle. \quad (6.11)$$

As explained above because of the matter effects on the way from the Sun center to its surface, $a_{\alpha i}^*$ is not in general equal to $\bar{a}_{\alpha i}$. It is straightforward to confirm that the oscillation probability for anti-neutrinos, $P(\bar{\nu}_\alpha \rightarrow \bar{\nu}_\mu)$, and its average are given by formulas respectively similar to Eqs. (6.4,6.8) replacing $a_{\alpha i}$ with $\bar{a}_{\alpha i}$ and $U_{\mu i}$ with $U_{\mu i}^*$.

Since the scattering cross sections of antineutrinos are smaller than that of neutrinos by a factor of about 2, their contribution to the events at the detector will be smaller.

Obviously, replacing μ with τ , we obtain the formula for $\langle P(\nu_\alpha \rightarrow \nu_\tau) \rangle_t^{t+\Delta t}$ and $\langle P(\bar{\nu}_\alpha \rightarrow \bar{\nu}_\tau) \rangle_t^{t+\Delta t}$. Notice that to the leading order in θ_{13} and $\theta_{23} - \pi/4$, $|U_{\mu i}| \simeq |U_{\tau i}|$ and $U_{\tau 1} U_{\tau 2}^* \simeq U_{\mu 1} U_{\mu 2}^*$. As a result, at this limit, $P(\nu_\alpha \rightarrow \nu_\tau)$ does not carry new information relative to $P(\nu_\alpha \rightarrow \nu_\mu)$. Muon-track events dominantly receive contributions from the CC interactions of ν_μ and $\bar{\nu}_\mu$. A subdominant contribution also comes from the CC interaction of ν_τ and the subsequent decay of tau to the muon which is suppressed by $\text{Br}(\tau \rightarrow \mu\nu\nu) \simeq 17\%$. As a result, up to a correction suppressed by $\text{Br}(\tau \rightarrow \mu\nu\nu) \sin \theta_{13}$, muon track events within interval $(t, t + \Delta t)$ from the sharp line is proportional to

$$K(t, \Delta t) \equiv \sum_\alpha n_\alpha \left(\langle P(\nu_\alpha \rightarrow \nu_\mu) \rangle_t^{t+\Delta t} + \frac{\sigma(\bar{\nu})}{\sigma(\nu)} \langle P(\bar{\nu}_\alpha \rightarrow \bar{\nu}_\mu) \rangle_t^{t+\Delta t} \right), \quad (6.12)$$

which should be added to the contribution from the continuous part of the spectrum. In general, the μ -track events can be written as

$$\mathcal{A} + \mathcal{B} K(t, \Delta t), \quad (6.13)$$

where \mathcal{A} comes from the continuous part of the spectrum. A priori, both \mathcal{A} and \mathcal{B} are unknown. While

$$\phi \equiv \Delta m_{12}^2 L / (2m_{DM}) \gg 2\pi,$$

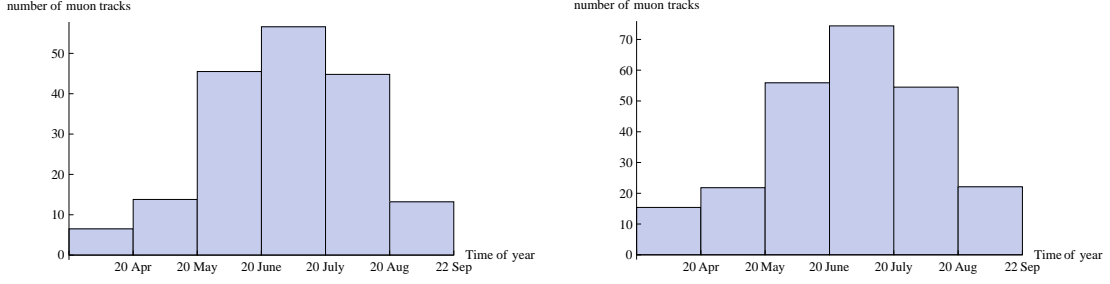


Figure 1. Number of the through-going μ -track events from the spring equinox (20 March) to autumn equinox (22 September) for $\theta_{13} = 0$ (left) and $\theta_{13} = 7^\circ$ (right). In drawing these histograms, we have assumed that DM particles with mass $m_{DM} = 270$ GeV decay via $DM+DM \rightarrow \nu_e \bar{\nu}_e$. For the DM capture rate in the Sun, we have taken $C_\odot = 3.4 \times 10^{22} \text{ s}^{-1}$.

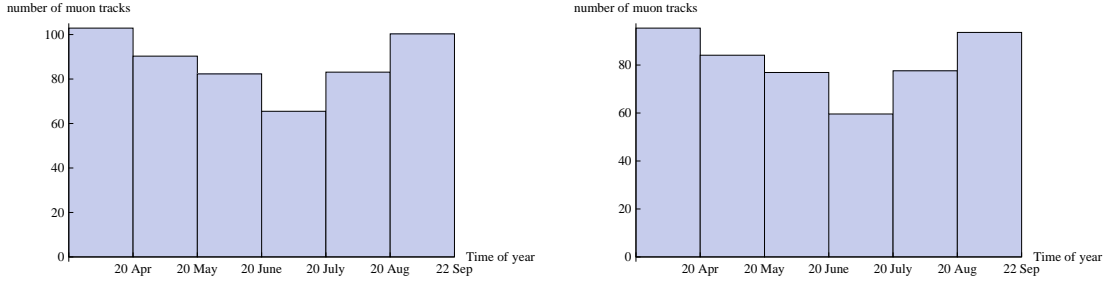


Figure 2. The same as figure 1 except that $DM+DM \rightarrow \nu_\mu \bar{\nu}_\mu$

the variation in ϕ due to seasonal change in the Sun Earth distance $\Delta L \sim 5 \times 10^6$ km is of the order of 2π . This means by studying the seasonal changes in muon track events, the ratio $\Delta m_{12}^2/m_{DM}$ can be derived.

Histograms in figures 1 and 2 display such seasonal changes for the case that DM pair dominantly annihilates into neutrino pairs. The horizontal axis shows the months between spring and autumn equinoxes during which neutrinos pass the Earth to reach the IceCube. As discussed in the previous section, during these months atmospheric muon background due to absorption by Earth is reduced and the data is therefore reliable. The peaks and dips in the histograms of figures 1 and 2 respectively correspond to the peaks and dips of the oscillation probabilities $P(\nu_e \rightarrow \nu_\mu)$ and $P(\nu_\mu \rightarrow \nu_\mu)$. If the present bound on the neutrino flux is saturated, after ten years of collecting data, the number of events during each month can amount to a few hundred so extracting $\Delta m_{12}^2/m_{DM}$ with a reasonable accuracy (about 10 %) would be possible. Since Δm_{12}^2 is already known, this ratio yields the DM mass. The value of the DM mass can in principle be derived by accelerators such as the LHC. If the two values coincide, it will be a noteworthy confirmation of the validity of the approach. In addition to $\Delta m^2/m_{DM}$, the seasonal variation also yields

$$\mathcal{A} + \mathcal{B} \sum_{\alpha} n_{\alpha} (|a_{\alpha i}|^2 |U_{\mu i}|^2 + \frac{\sigma(\bar{\nu})}{\sigma(\nu)} |\bar{a}_{\alpha i}|^2 |U_{\mu i}|^2), \quad (6.14)$$

as well as

$$\mathcal{B} \left| \sum_{\alpha} n_{\alpha} \left(a_{\alpha 1}^* a_{\alpha 2} U_{\mu 1} U_{\mu 2}^* + \frac{\sigma(\bar{\nu})}{\sigma(\nu)} \bar{a}_{\alpha 1}^* \bar{a}_{\alpha 2} U_{\mu 1}^* U_{\mu 2} \right) \right|. \quad (6.15)$$

Moreover, the seasonal variation yields the following combination of ϕ , $\arg[a_{\alpha 1}^* a_{\alpha 2}]$ and $\arg[\bar{a}_{\alpha 1}^* \bar{a}_{\alpha 2}]$:

$$\arg \left[\sum_{\alpha} n_{\alpha} \left(a_{\alpha 1}^* a_{\alpha 2} U_{\mu 1} U_{\mu 2}^* + \frac{\sigma(\bar{\nu})}{\sigma(\nu)} \bar{a}_{\alpha 1}^* \bar{a}_{\alpha 2} U_{\mu 1}^* U_{\mu 2} \right) \right] + \phi. \quad (6.16)$$

Since $\phi/(2\pi) \sim 25(200 \text{ GeV}/m_{DM})$, to derive meaningful information on $\arg[a_{\alpha 1}^* a_{\alpha 2}]$ and $\arg[\bar{a}_{\alpha 1}^* \bar{a}_{\alpha 2}]$, ϕ has to be known with percent level accuracy or better which does not seem to be achievable in foreseeable future. To derive these four independent pieces of information (i.e., $\Delta m_{12}^2/m_{DM}$ and three combinations in eqs. (6.14, 6.15, 6.16)), one can divide the time period between two equinoxes to four segments and measure the number of μ -tracks in each interval. If the number of events at each interval exceeds a few 100, the statistics will be enough to perform the analysis and derive the aforementioned combinations with about 10 % accuracy.

Notice that the density matrix in eq. (6.1) (or equivalently matrix $\bar{\rho}$ in eq. (6.10)) contains seven free parameters: three real values of n_{α} and four parameters (3 angles + 1 phase) determining ν'_{α} in the flavor basis. Of course, the three combinations that can be extracted are not enough to reconstruct ρ (and therefore $\mathcal{M}_{\alpha\beta}$). However, these three combinations yield valuable insight on the flavor structure of $\rho_{\alpha\beta}$ and therefore $\mathcal{M}_{\alpha\beta}$. In the following, we discuss the additional information that can be derived from the shower-like events.

As is well-known, shower-like events receive contribution from three sources: (1) universal NC interaction of all neutrino species which is insensitive to neutrino oscillation probability because $\sum_{\beta} P(\nu_{\alpha} \rightarrow \nu_{\beta}) = \sum_{\beta} P(\bar{\nu}_{\alpha} \rightarrow \bar{\nu}_{\beta}) = 1$; (2) CC interactions of ν_e and $\bar{\nu}_e$ whose contributions are given by $P(\nu_{\alpha} \rightarrow \nu_e) + P(\bar{\nu}_{\alpha} \rightarrow \bar{\nu}_e)\sigma(\bar{\nu}_e)/\sigma(\nu_e)$; (3) CC interactions of ν_{τ} and $\bar{\nu}_{\tau}$ and the subsequent hadronic decay of τ whose effect is given by $[1 - \text{Br}(\tau \rightarrow \mu\nu\nu)][P(\nu_{\alpha} \rightarrow \nu_{\tau}) + P(\bar{\nu}_{\alpha} \rightarrow \bar{\nu}_{\tau})\sigma(\bar{\nu}_{\tau})/\sigma(\nu_{\tau})]$. Remember that up to a correction of the order of $\text{Max}[\theta_{13}, \theta_{23} - \pi/4]$, $P(\nu_{\alpha}^{(-)} \rightarrow \nu_{\mu}^{(-)}) \simeq P(\nu_{\alpha}^{(-)} \rightarrow \nu_{\tau}^{(-)})$. One can write the shower-like events as

$$\mathcal{C} - r\mathcal{B}K(t, \Delta t), \quad (6.17)$$

where $K(t, \Delta t)$ is defined in eq. (6.12) and r is a calculable quantity (see section 4). The quantity \mathcal{C} receives contribution both from continuous part of the spectrum and the sharp line. Combining the number of shower-like events with the information derived from the seasonal variation of the μ -track events yields $\mathcal{C} + r\mathcal{A}$. In principle, \mathcal{C} can be predicted from \mathcal{A} and \mathcal{B} but for such a prediction, knowledge of the shape of the spectrum is required which to some extent can be extracted from energy measurements. In fact, for a given value of m_{DM} , the shape of continuous spectrum from various annihilation modes such as $\text{DM} + \text{DM} \rightarrow b\bar{b}, \tau\bar{\tau}, ZZ, W^+W^-$ can be determined. The shape of spectrum for scattered and regenerated neutrinos from $\text{DM} + \text{DM} \rightarrow \nu\nu$ can be also determined. In other words, \mathcal{C} depends on the relative ratios of the different annihilation modes. Such an analysis might provide a cross-check for the consistency of the analysis and the measurements. For further study of the role of R in determining the decay modes see ref. [24].

7 Illustrative examples

From the theoretical point of view, the neutrino states produced inside the Sun do not need to coincide with any of flavor eigenstates as the flavor structure of the physics governing the DM sector might be different from the physics determining the flavor structure of the SM. However, for illustrative purposes in this section, we study the case that the neutrino state at production corresponds to ν_e , ν_μ or ν_τ . In other words, we assume ρ and $\bar{\rho}$ at production to be flavor diagonal. Remember that the study applies both to $\text{DM} + \text{DM} \rightarrow \nu_\alpha + \nu_\alpha, \bar{\nu}_\alpha + \bar{\nu}_\alpha$ and $\text{DM} + \text{DM} \rightarrow \nu_\alpha + \bar{\nu}_\alpha$.

At the production point, the matter effect $\sqrt{2}G_F n_e$ is much larger than $\Delta m_{12}^2/(2E)$ so $|\nu_e\rangle$ and $|\bar{\nu}_e\rangle$ will respectively correspond to $|\nu_2\rangle$ and $|\bar{\nu}_1\rangle$. As $|\nu_e\rangle$ propagates outside, it will reach the 12-resonance region. At these energies, the transition is non-adiabatic so at the surface $|a_{e1}| \sim |a_{e2}|$. For the case of antineutrinos, there is no such resonance region so at the surface $|\bar{a}_{e1}| \gg |\bar{a}_{e2}|$. For normal hierarchical scheme and nonzero θ_{13} , neutrinos will undergo a second resonance. For θ_{13} within the reach of the forthcoming experiments [23] (i.e., $\theta_{13} > 7^\circ$), this resonance is also non-adiabatic. For inverted hierarchical scheme, instead of neutrinos, antineutrinos will undergo the resonance due to the 13-splitting.

For lower values of the DM mass, detection rate becomes smaller as the neutrino-nuclei cross section decreases with lowering the energies of neutrinos. On the other hand, with increasing m_{DM} , the sharp line composed of the unscattered neutrinos diminishes, leading to a suppressed Δ . It can be shown that for $m_{DM} \gtrsim 500$ GeV, the tail of the spectrum from the scattered neutrinos suppresses Δ down to values $\Delta \lesssim 0.5$. Thus, generally we expect that in the range, $100 \text{ GeV} < m_{DM} < 500 \text{ GeV}$, the Δ measurement method will be most useful. We focus on $m_D \simeq 200$ GeV and study the high sensitivity of Δ to m_{DM} . We have checked for other values of m_{DM} in the range 100 GeV to 300 GeV and found that our results are robust against varying m_{DM} . Using the code described in section 5, we have calculated the seasonal variation, R_{DC} and R_{thr} for $m_{DM} = 197, 200, 203$ GeV, $\theta_{13} = 0, 7^\circ$ and $\delta = 0, \pi/2, \pi$, taking the initial neutrino flavor to be ν_e , ν_μ and ν_τ . The results are displayed in tables 1, 2 and 3.

For the shower-like events, the effective volume of a detector is approximately equal to its geometrical volume: $V_{eff}^{shower} = dA_{eff}$ where d and A_{eff} are respectively the depth and effective area of the detector. However, since the muons can penetrate farther, the effective volume for their detection can be larger: $V_{eff}^\mu = (R_\mu + d)A_{eff}$ where R_μ is the muon range which depends only on the chemical composition of the medium. As a result, the ratio of μ -track to shower-like events is enhanced by a factor of $(R_\mu + d)/d$. Obviously, for a smaller detector this enhancement factor is larger. That is why the ratio in the case of Deepcore, R_{DC} , is so much larger than the ratio in the case of the whole detector, R_{thr} . (See tables 1, 2 and 3.)

The matter effects inside the Sun do not distinguish between ν_μ and ν_τ . Thus, if the neutrino mass matrix is $\mu\tau$ -symmetric in vacuum (i.e., $\theta_{13} = \theta_{23} - \pi/4 = 0$), the neutrino sector remains $\mu\tau$ -symmetric in the matter. This means that in this limit, regardless of whether neutrino mass scheme is normal or inverted, we can write

$$|\nu_e; \text{surface}\rangle = \cos \theta_{12}^s |1\rangle + \sin \theta_{12}^s |2\rangle, \quad (7.1)$$

$$|\nu_\mu; \text{surface}\rangle = -\frac{\sin \theta_{12}^s}{\sqrt{2}} |1\rangle + \frac{\cos \theta_{12}^s}{\sqrt{2}} |2\rangle + \frac{1}{\sqrt{2}} |3\rangle \quad (7.2)$$

m_{DM}	N/I	θ_{13}	δ	R^{IC}	R^{DC}	Δ_{20Mar}^{IC}	Δ_{3Apr}^{IC}	Δ_{20Mar}^{DC}	Δ_{3Apr}^{DC}
197	N	0	0	0.4	14	0.7	0.7	0.7	0.7
197	I	0	0	0.4	14	0.7	0.7	0.7	0.7
197	N	7°	0	0.5	18	0.5	0.6	0.6	0.6
197	I	7°	0	0.6	20	0.6	0.6	0.6	0.6
197	N	7°	$\pi/2$	0.5	18	0.5	0.5	0.5	0.5
197	I	7°	$\pi/2$	0.6	19	0.5	0.5	0.5	0.5
197	N	7°	π	0.4	14	0.6	0.6	0.6	0.6
197	I	7°	π	0.5	16	0.4	0.5	0.4	0.5
200	N	0	0	0.5	15	0.5	0.5	0.5	0.5
200	I	0	0	0.5	15	0.5	0.5	0.5	0.5
200	N	7°	0	0.6	19	0.4	0.5	0.4	0.4
200	I	7°	0	0.7	22	0.4	0.4	0.3	0.4
200	N	7°	$\pi/2$	0.6	17	0.4	0.5	0.4	0.4
200	I	7°	$\pi/2$	0.7	19	0.4	0.4	0.4	0.4
200	N	7°	π	0.5	14	0.4	0.4	0.4	0.4
200	I	7°	π	0.5	15	0.4	0.4	0.4	0.4
203	N	0	0	0.5	15	0.1	0.2	0.2	0.2
203	I	0	0	0.5	15	0.1	0.2	0.1	0.2
203	N	7°	0	0.6	19	0.1	0.1	0.2	0.2
203	I	7°	0	0.7	20	0.1	0.1	0.1	0.1
203	N	7°	$\pi/2$	0.6	19	0.0	0.0	0.1	0.1
203	I	7°	$\pi/2$	0.6	19	0.0	0.1	0.1	0.1
203	N	7°	π	0.5	15	0.1	0.1	0.2	0.2
203	I	7°	π	0.6	17	0.1	0.1	0.2	0.2

Table 1. Seasonal variation and μ -track to shower-like ratio for DM particles with mass m_{DM} (in GeV) and annihilation mode $DM + DM \rightarrow \nu_e \nu_e$. N/I indicates normal versus inverted neutrino mass scheme. R^{IC} indicates the ratio of the numbers of muon-track to shower-like event for through-going events measured by the whole IceCube. R^{DC} is the same quantity measured by DeepCore. Δ_{20Mar} is the seasonal variation between two equinoxes $\Delta_{20Mar} \equiv \Delta(20 \text{ Mar}, 186 \text{ days}, 23 \text{ Sep}, 179 \text{ days})$. Finally, $\Delta_{3Apr} \equiv \Delta(3 \text{ Apr}, 186 \text{ days}, 6 \text{ Oct}, 179 \text{ days})$. See eqs. (2.1, 4.2, 4.4).

and

$$|\nu_\tau; \text{surface}\rangle = \frac{\sin \theta_{12}^s}{\sqrt{2}}|1\rangle - \frac{\cos \theta_{12}^s}{\sqrt{2}}|2\rangle + \frac{1}{\sqrt{2}}|3\rangle. \quad (7.3)$$

Notice that θ_{12}^s is different from θ_{12} mixing angle in the U_{MNS} neutrino mixing matrix. Similar relations holds for antineutrinos but with a different value of $\bar{\theta}_{12}^s$. For antineutrinos, we expect $\cos \bar{\theta}_{12}^s \simeq 1$. In terms of the notation in eqs. (6.2, 6.11), $a_{e1} = \cos \theta_{12}^s$, $\bar{a}_{e1} = \cos \bar{\theta}_{12}^s$, $a_{e3} = \bar{a}_{e3} = 0$, $a_{\mu 3} = \bar{a}_{\mu 3} = a_{\tau 3} = \bar{a}_{\tau 3} = 1/\sqrt{2}$ and etc. From the above relations we find $|a_{\mu i}^{(-)}| = |a_{\tau i}^{(-)}|$, $a_{\mu 1}^* a_{\mu 2} U_{\mu 1}^* U_{\mu 2}^* = a_{\tau 1}^* a_{\tau 2} U_{\mu 1}^* U_{\mu 2}^*$ and $\bar{a}_{\mu 1}^* \bar{a}_{\mu 2} U_{\mu 1}^* U_{\mu 2}^* = \bar{a}_{\tau 1}^* \bar{a}_{\tau 2} U_{\mu 1}^* U_{\mu 2}^*$. Notice however that $a_{\mu 1}^* a_{\mu 2} U_{\mu 1}^* U_{\mu 2}^* \neq a_{\tau 1}^* a_{\tau 3} U_{\mu 1}^* U_{\mu 3}^*$. Thus, in the $\mu\tau$ -symmetric case, up to the corrections of order of O_{13} (see eq. (6.7) for the definition), $\langle P(\nu_\mu \rightarrow \nu_\mu) \rangle \simeq \langle P(\nu_\tau \rightarrow \nu_\mu) \rangle$ and $\langle P(\bar{\nu}_\mu \rightarrow \bar{\nu}_\mu) \rangle \simeq \langle P(\bar{\nu}_\tau \rightarrow \bar{\nu}_\mu) \rangle$. This means, to leading approximation, if we take only the unscattered neutrinos, the contribution to Δ and R will be the same for initial ν_μ and ν_τ . This makes distinguishing between $(DM+DM \rightarrow \nu_\mu \nu_\mu)$ and $(DM+DM \rightarrow \nu_\tau \nu_\tau)$ difficult. However,

m_{DM}	N/I	θ_{13}	δ	R^{IC}	R^{DC}	Δ_{20Mar}^{IC}	Δ_{3Apr}^{IC}	Δ_{20Mar}^{DC}	Δ_{3Apr}^{DC}
197	N	0	0	1.0	47	0.1	0.1	0.0	0.1
197	I	0	0	1.0	48	0.1	0.1	0.0	0.1
197	N	7°	0	0.9	42	0.1	0.1	0.1	0.1
197	I	7°	0	0.9	42	0.1	0.1	0.1	0.1
197	N	7°	$\pi/2$	0.9	44	0.1	0.1	0.1	0.1
197	I	7°	$\pi/2$	1.0	48	0.0	0.0	0.0	0.0
197	N	7°	π	1.0	51	0.0	0.0	0.0	0.0
197	I	7°	π	1.0	50	0.0	0.0	0.0	0.0
200	N	0	0	1.0	49	0.1	0.1	0.1	0.1
200	I	0	0	1.0	47	0.1	0.1	0.0	0.0
200	N	7°	0	0.9	43	0.1	0.1	0.05	0.05
200	I	7°	0	0.8	41	0.1	0.2	0.1	0.1
200	N	7°	$\pi/2$	0.9	46	0.1	0.1	0.1	0.1
200	I	7°	$\pi/2$	1.0	48	0.1	0.1	0.0	0.0
200	N	7°	π	1.0	52	0.1	0.1	0.1	0.1
200	I	7°	π	1.0	50	0.0	0.0	0.0	0.0
203	N	0	0	1.0	50	0.0	0.0	0.0	0.0
203	I	0	0	1.1	52	0.0	0.0	0.0	0.0
203	N	7°	0	0.9	45	0.1	0.1	0.0	0.1
203	I	7°	0	1.0	46	0.1	0.1	0.1	0.1
203	N	7°	$\pi/2$	1.0	47	0.0	0.0	0.0	0.0
203	I	7°	$\pi/2$	1.1	52	0.0	0.0	0.0	0.0
203	N	7°	π	1.1	54	0.0	0.0	0.0	0.0
203	I	7°	π	1.0	52	0.1	0.1	0.0	0.0

Table 2. The same as Table 1 for $DM+DM \rightarrow \nu_\mu \nu_\mu$.

the regenerated neutrinos coming from $\nu_\tau \rightarrow \tau \rightarrow \nu_\tau$ in the Sun differentiate between them. Remember that at these energies $\Delta m_{13}^2 R_\odot / 2E < 2\pi$. In fact, ν_μ can only partially oscillate to ν_τ before exiting the Sun. Thus, the contribution to regenerated neutrinos strongly depends on the initial flavor of the neutrino. Of course the regenerated neutrinos will have less energy, so they are more important for DeepCore than the whole IceCube because the energy threshold of DeepCore is lower. Our results show that for $\theta_{13} = \theta_{23} - \pi/4 = 0$, the deviations of Δ^{IC} and R^{IC} for initial ν_μ from the same quantities for initial ν_τ are negligible (compare tables 2 and 3). As seen from the tables, this deviation for the case measured by the DeepCore (i.e., Δ^{DC} and R^{IC}) is larger. This can be explained by the contribution from the regenerated neutrinos.

Another point to note is that since the validity of eq. (7.1) does not depend on scheme, we expect that for $\theta_{13} = 0$ and initial ν_e , Δ and R to be the same for normal and inverted mass schemes. Results shown in table 1 confirm this expectation.

The tables show that the sensitivity of Δ to m_{DM} is very high. As discussed in the previous section and shown in figure 1, by studying the variation over four intervals of time, $\Delta m_{12}^2 / m_{DM}$ can be derived.

From the tables we observe that for $(DM+DM \rightarrow \nu_e + \nu_e)$, Δ can be significant; however, for the cases $(DM + DM \rightarrow \nu_\mu + \nu_\mu)$ and $(DM + DM \rightarrow \nu_\tau + \nu_\tau)$, Δ is in general small. We

m_{DM}	N/I	θ_{13}	δ	R^{IC}	R^{DC}	Δ_{20Mar}^{IC}	Δ_{3Apr}^{IC}	Δ_{20Mar}^{DC}	Δ_{3Apr}^{DC}
197	N	0	0	1.1	65	0.1	0.1	0.1	0.1
197	I	0	0	1.1	65	0.1	0.1	0.1	0.1
197	N	7°	0	1.0	59	0.1	0.1	0.1	0.1
197	I	7°	0	1.0	57	0.1	0.1	0.1	0.1
197	N	7°	$\pi/2$	1.1	64	0.1	0.1	0.1	0.1
197	I	7°	$\pi/2$	1.0	59	0.1	0.1	0.1	0.1
197	N	7°	π	1.1	68	0.1	0.1	0.1	0.1
197	I	7°	π	1.1	66	0.1	0.1	0.0	0.1
200	N	0	0	1.1	66	0.1	0.1	0.0	0.0
200	I	0	0	1.1	67	0.1	0.1	0.0	0.0
200	N	7°	0	1.0	59	0.1	0.1	0.0	0.0
200	I	7°	0	1.0	58	0.0	0.0	0.0	0.0
200	N	7°	$\pi/2$	1.1	65	0.0	0.0	0.0	0.0
200	I	7°	$\pi/2$	1.0	61	0.1	0.1	0.0	0.0
200	N	7°	π	1.1	70	0.0	0.0	0.0	0.0
200	I	7°	π	1.1	69	0.1	0.1	0.0	0.0
203	N	0	0	1.1	67	0.0	0.0	0.0	0.0
203	I	0	0	1.0	66	0.0	0.0	0.0	0.0
203	N	7°	0	1.0	60	0.0	0.0	0.0	0.0
203	I	7°	0	0.9	58	0.1	0.1	0.0	0.0
203	N	7°	$\pi/2$	1.0	66	0.0	0.0	0.0	0.0
203	I	7°	$\pi/2$	0.9	61	0.0	0.0	0.0	0.0
203	N	7°	π	1.1	71	0.0	0.0	0.0	0.0
203	I	7°	π	1.0	69	0.0	0.0	0.0	0.0

Table 3. The same as Table 1 for $DM+DM \rightarrow \nu_\tau \nu_\tau$.

found that this observation is robust against varying m_{DM} . The reason is two folded: (i) For initial ν_μ and ν_τ , the contribution from the continuous regenerated neutrinos to the flux at the detector is higher so the denominator of the ratio in eq. (2.1) is enhanced leading to lower values of Δ . From tables 2 and 3, we observe that Δ^{DC} is smaller than Δ^{IC} . The reason is that DeepCore has a lower detection threshold so it receives a larger contribution from regenerated neutrinos which are in general less energetic. (ii) The second reason is that for $\alpha = \mu, \tau$; $a_{\alpha 1} a_{\alpha 2} U_{\mu 1} U_{\mu 2}$ is smaller (see eq. (6.8)). However, we should remember that $(DM+DM \rightarrow \nu_\mu + \nu_\mu)$ and $(DM+DM \rightarrow \nu_\tau + \nu_\tau)$ are quite specific cases. In general DM pair can annihilate to general coherent combinations of the different neutrino flavors for which Δ is in general large.

8 Conclusion and discussion

We have shown that by studying the time variation of μ -track events, valuable information on the nature of DM particles can be derived: (i) Measuring a nonzero value for Δ defined in eq. (2.1) implies that there is a sharp monochromatic feature in the neutrino spectrum which in turn means $DM + DM \rightarrow \nu + \nu$ is [one of] the significant annihilation modes. (ii) Once such a feature is established, by studying the μ -track events over four different time intervals,

the value of $\Delta m_{12}^2/m_{DM}$ as well as three independent combinations (see eqs. (6.14,6.15,6.16) as well as eq. (6.13)) of $a_{\alpha i}$ and $\bar{a}_{\alpha j}$ which are defined in eqs. (6.2,6.11) can be extracted. Thus, by this method, m_{DM} can be extracted and checked against the value derived from studying the endpoint of the spectrum or from the accelerator experiments. Although the information will not be enough to completely reconstruct the flavor structure of the amplitude of $DM + DM \rightarrow \nu_\alpha + \nu_\beta$, the combinations in eqs. (6.14) and (6.15) contain invaluable information that can constrain models predicting $DM + DM \rightarrow \nu_\alpha + \nu_\beta$. In particular, observing nonzero oscillatory effects rules out models predicting democratic neutrino flavor production. Moreover, our numerical results show that by studying Δ , models predicting $DM + DM \rightarrow \nu_e + \nu_e^{(-)}$ can be distinguished from those predicting $DM + DM \rightarrow \nu_\mu + \nu_\mu^{(-)}$ or $DM + DM \rightarrow \nu_\tau + \nu_\tau^{(-)}$. Notice that to derive information on $\mathcal{M}_{\alpha\beta}$ from $a_{\alpha i}$, the evolution of the neutrino state from the Sun center to its surface has to be taken into account. This can be readily done by codes such as the one developed to derive the numerical results of the present paper (see, tables 1, 2, 3).

We showed that it is possible that while DM particles dominantly annihilate into neutrino pairs, their interaction rate with nuclei in the Sun is high enough to lead to high enough DM capture rate and therefore to a neutrino flux saturating the present bounds. If the present bound on the neutrino flux from dark matter annihilation is saturated, after about 10 years of data taking, the statistics will be high enough to make this method reliable. In this method, only μ -track events are employed so high energy threshold for the detection of shower-like events will not be a hinderance. To carry out this analysis, it will be enough to take data from 20th of March to 23rd of September when the neutrino from the Sun pass through the Earth to reach the detector and as a result, the atmospheric muon background will not be a problem. The method presented in this paper can be combined with the energy spectrum measurements [6] and the ratio of μ -track to shower-like events [24] to draw a more complete picture of the dark matter annihilation modes.

Acknowledgments

We are grateful to R. Allahverdi and K. Richardson-McDaniel for useful discussion through which the idea of this paper was born as well as for collaborating at the early stages of this work. We would also like to thank M. Blennow and T. Ohlsson for useful discussions. We specially appreciate Prof. F. Halzen for his encouragements. A. E. appreciates “Bonyad-e-Melli-e-Nokhbegan” in Iran and the Brazilian funding agency Fundação de Amparo à Pesquisa do Estado de São Paulo (FAPESP) for partial financial support.

References

- [1] A. Esmaili and Y. Farzan, Phys. Rev. D **81** (2010) 113010 [arXiv:0912.4033 [hep-ph]].
- [2] M. Lindner, A. Merle and V. Niro, arXiv:1005.3116 [hep-ph].
- [3] G. L. Fogli, E. Lisi, A. Mirizzi, D. Montanino and P. D. Serpico, Phys. Rev. D **74** (2006) 093004 [arXiv:hep-ph/0608321].
- [4] M. Honda, T. Kajita, K. Kasahara *et al.*, Phys. Rev. **D75** (2007) 043006. [astro-ph/0611418].
- [5] V. Barger, J. Kumar, D. Marfatia *et al.*, Phys. Rev. **D81** (2010) 115010. [arXiv:1004.4573 [hep-ph]].

- [6] M. Cirelli, N. Fornengo, T. Montaruli, I. Sokalski, A. Strumia and F. Vissani, Nucl. Phys. B **727**, 99 (2005) [Erratum-ibid. B **790**, 338 (2008)] [arXiv:hep-ph/0506298]. (See the archive version.)
- [7] V. D. Barger, W. Y. Keung and G. Shaughnessy, Phys. Lett. B **664** (2008) 190 [arXiv:0709.3301 [astro-ph]]; A. E. Erkoca, M. H. Reno, I. Sarcevic, Phys. Rev. D **80** (2009) 043514. [arXiv:0906.4364 [hep-ph]]; D. Hooper and G. D. Kribs, Phys. Rev. D **67** (2003) 055003 [arXiv:hep-ph/0208261]; R. Lehnert and T. J. Weiler, Phys. Rev. D **77**, 125004 (2008) [arXiv:0708.1035 [hep-ph]]; R. Lehnert and T. J. Weiler, arXiv:1002.2441 [hep-ph]; M. Blennow, H. Melbeus and T. Ohlsson, JCAP **1001** (2010) 018 [arXiv:0910.1588 [hep-ph]]; V. Niro, A. Bottino, N. Fornengo and S. Scopel, Phys. Rev. D **80** (2009) 095019 [arXiv:0909.2348 [hep-ph]].
- [8] M. Blennow, J. Edsjo and T. Ohlsson, JCAP **0801** (2008) 021 [arXiv:0709.3898 [hep-ph]].
- [9] V. Barger, W. Y. Keung, G. Shaughnessy and A. Tregre, Phys. Rev. D **76** (2007) 095008 [arXiv:0708.1325 [hep-ph]].
- [10] Y. Farzan, Phys. Rev. D **80**, 073009 (2009) [arXiv:0908.3729 [hep-ph]]; C. Boehm, Y. Farzan, T. Hambye, S. Palomares-Ruiz and S. Pascoli, Phys. Rev. D **77**, 043516 (2008) [arXiv:hep-ph/0612228]; Y. Farzan, S. Pascoli, M. A. Schmidt, [arXiv:1005.5323 [hep-ph]].
- [11] G. Jungman, M. Kamionkowski and K. Griest, Phys. Rept. **267**, 195 (1996) [arXiv:hep-ph/9506380].
- [12] E. Aprile *et al.* [XENON100 Collaboration], Phys. Rev. Lett. **105** (2010) 131302. [arXiv:1005.0380 [astro-ph.CO]]; C. E. Aalseth *et al.* [CoGeNT Collaboration], [arXiv:1002.4703 [astro-ph.CO]]; Z. Ahmed *et al.* [The CDMS-II Collaboration], Science **327** (2010) 1619-1621. [arXiv:0912.3592 [astro-ph.CO]]; J. Angle *et al.* [XENON10 Collaboration], Phys. Rev. D **80** (2009) 115005. [arXiv:0910.3698 [astro-ph.CO]]; E. Armengaud, C. Augier, A. Benoit *et al.*, Phys. Lett. B **687** (2010) 294-298. [arXiv:0912.0805 [astro-ph.CO]]; V. N. Lebedenko *et al.*, Phys. Rev. D **80** (2009) 052010 [arXiv:0812.1150 [astro-ph]].
- [13] J. Ahrens *et al.* [IceCube Collaboration], Astropart. Phys. **20** (2004) 507-532. [astro-ph/0305196].
- [14] J. Ahrens *et al.* [AMANDA Collaboration], Phys. Rev. D **66** (2002) 012005. [astro-ph/0205109].
- [15] A. Esmaili, Y. Farzan, Nucl. Phys. B **821** (2009) 197-214. [arXiv:0905.0259 [hep-ph]].
- [16] D. E. Groom, N. V. Mokhov, S. I. Striganov, Atom. Data Nucl. Data Tabl. **78** (2001) 183-356.
- [17] M. C. Gonzalez-Garcia, F. Halzen, S. Mohapatra, Astropart. Phys. **31** (2009) 437-444. [arXiv:0902.1176 [astro-ph.HE]].
- [18] C. Wiebusch and f. t. I. Collaboration, arXiv:0907.2263 [astro-ph.IM].
- [19] E. Resconi, f. t. I. Collaboration, Nucl. Instrum. Meth. A **602** (2009) 7-13. [arXiv:0807.3891 [astro-ph]].
- [20] J. N. Bahcall, A. M. Serenelli, S. Basu, Astrophys. J. **621** (2005) L85-L88. [astro-ph/0412440].
- [21] R. Gandhi, C. Quigg, M. H. Reno and I. Sarcevic, Phys. Rev. D **58** (1998) 093009 [arXiv:hep-ph/9807264].
- [22] L. Pasquali and M. H. Reno, Phys. Rev. D **59** (1999) 093003 [arXiv:hep-ph/9811268]; P. Lipari, Astropart. Phys. **1** (1993) 195.
- [23] X. Guo *et al.* [Daya-Bay Collaboration], arXiv:hep-ex/0701029; F. Ardellier *et al.* [Double Chooz Collaboration], arXiv:hep-ex/0606025.
- [24] R. Allahverdi and K. Richardson-McDaniel, *Prospects for extracting dark matter parameters from neutrino telescopes*, work in progress.